Thioglycerol-functionalized CdSe quantum dots detecting cadmium ions

Nassim Ben Brahim, Naim Bel Haj Mohamed, Mosaab Echabaane, Mohamed Haouari, Rafik Ben Chaâbane, Michel Negrerie, Hafedh Ben Ouada

Thioglycerol-functionalized CdSe quantum dots detecting cadmium ions

Nassim Ben Brahim[a,*], Naim Bel Haj Mohamed[a], Mosaab Echabaane[a], Mohamed Haouari[a], Rafik Ben Chaâbane[a], Michel Negrerie[b,*] and Hafedh Ben Ouada[a]

[a]*Laboratoire des Interfaces et Matériaux Avancés, Faculté des Sciences de Monastir, Bd. de l'Environnement, 5019 Monastir, Tunisia.*
[b]*Laboratoire d'Optique et Biosciences, INSERM U1182, CNRS UMR7645, Ecole Polytechnique, 91128 Palaiseau, France.*

*Corresponding authors.
E-mail: nassim.benbrahim.fsm@gmail.com. Phone: +216 96 400 499
E-mail: michel.negrerie@polytechnique.fr. Phone: +331 69 33 50 52

Keywords:
CdSe quantum dots synthesis
Absorption spectroscopy
Electronic microscopy
Cadmium detection
Cation binding selectivity

Highlights:

- Water-soluble CdSe quantum dots capped with thioglycerol were synthesized.
- The absorption spectrum of the quantum dots dramatically changes upon cadmium binding.
- The presence of 17 other metal ions does not change the spectrum TG-CdSe quantum dots.
- The specificity of these CdSe thioglycerol-capped quantum dots for Cd^{2+} is very high.

ABSTRACT

Water-soluble CdSe quantum dots (QDs) were synthesized using thioglycerol (TG) as the surface capping agent through a one-step process at low temperature T (100°C). The CdSe quantum dots were characterized by X-ray diffraction, Fourier transform infrared spectroscopy, transmission electron microscopy, UV-visible absorption and fluorescence spectroscopies. These measurements revealed that the TG-capped CdSe QDs possess a high crystalline quality with an average diameter in the range 2.5 – 2.8 nm and exhibit particular optical properties. The UV-visible absorption of CdSe QDs is enhanced by the addition of cadmium ions, with a simultaneous shift of the edge band (400 nm), while seventeen other tested metal cations have no effect on the absorption of QDs. Moreover, the binding of Cd^{2+} ions induces a quenching of the fluorescence emission of TG-CdSe QDs. At particular absorption wavelengths, the response is linearly proportional to the cadmium ions concentration ranging from 1.0 to 22 µM with a detection limit of 0.32 µM (37 $\mu g \cdot L^{-1}$). Based on these optical properties, the TG-CdSe QDs could be used as a highly selective probe for the detection of Cd^{2+} ions in aqueous solutions, a species highly toxic for cells.

1. Introduction

Quantum dots (QDs), or semiconductor nanocrystals, are nowadays inestimable tools for fundamental studies as well as for potential applications such as biological probes [1,2], fluorescent biosensor [3], light-emitting diodes (LEDs) [4] and solar cells [5]. Compared to conventional organic dyes, QDs possess unique properties including continuous absorption band, high photoluminescence (PL) quantum yields, photobleaching stability and tunability of the PL emission as a function of their size [6,7]. To date, two different routes have been reported for the synthesis of CdSe QDs, one being the most conventional organometallic approach [8,9]. As prepared, the CdSe nanocrystals have remarkable properties such as narrow width of the PL spectrum, high PL quantum yield, negligible photobleaching and excellent size homogeneity. This non-aqueous synthesis of capped QDs requires high temperature (360 °C) [10], use of hydrophobic ligands [11] and solubilization strategies for their direct use in biological systems [12]. Alternatively, the aqueous synthesis route produces QDs with other advantages, including control of the size by the pH [13], water solubility, biological compatibility and stability [14,15]. However, the aqueous method has several drawbacks such as lower emission efficiency and a wider PL spectrum compared to the organic method. The design and synthesis of high quality water-soluble CdSe QDs disclosing specific and tunable properties to target biochemical analytes or biomolecular systems is a major issue, mainly reached by the choice of the functionalizing ligand coupled to CdSe. For example, Xue *et al.* reported highly luminescent water-soluble CdSe QDs prepared using thioglycolic acid as a capping ligand, which were covalently coupled to bacteria [16]. Alternatively, particular capped CdSe QDs could be prepared at the polarizable interface between water and 1,2-dichloroethane electrolyte solutions by an electrochemical method [17]. Triethanolamine-capped CdSe QDs were synthesized and used as fluorescent sensors for

reciprocal recognition of mercury and iodide in aqueous solution [18] and CdSe nanocrystals incorporated in thin films were shown to interact with gazeous compounds such as benzylamine and triethylamine [19].

Here, we focus on the detection of cadmium ions, which is an extremely toxic metal widely found in plastics, fossil fuel combustion, phosphate fertilizers and other various chemicals [20]. These sources of cadmium often lead to contaminations in water, soil and eventually in food [21,22], causing serious environmental and health problems such as lung, prostate damage and kidney cancer [23,24]. In this study, we report the synthesis of thioglycerol-capped CdSe QDs and its interaction with cadmium in water. A facile preparation through a seed-assisted method at room temperature yields water-soluble CdSe QDs capped with thioglycerol (TG) which was used for the detection of Cd^{2+} ion by UV-Visible spectroscopy. These CdSe functionalized nanoparticles are characterized by a simple and low-cost preparation and a remarkably high selectivity for Cd^{2+} ions.

2. Experimental procedures

2.1. Synthesis of TG-capped CdSe QDs

We have followed the method previously described for the synthesis of CdS (cadmium sulfure) QDs capped with thiol derivatives [25] with some modifications. The chemicals were purchased from Sigma, Aldrich and Fluka. Briefly, an aqueous solution was obtained by mixing cadmium acetate dehydrate with thioglycerol (TG) as the stabilizer in deionized water with continuous stirring under nitrogen atmosphere. The pH of the resultant mixture was adjusted to 11.2 with NaOH solution. Separately, an aqueous solution of Na_2SeO_3 was prepared by introducing SeO_2 into a NaOH solution and injected into the pH-controled

mixture of Cd^{2+} and stabilizer under vigorous stirring. The molar ratio Cd^{2+}/TG/Se^{2-} was set at 1/2/0.5. Then, a solution of the reducing agent $NaBH_4$ was injected with a syringe to the final solution under continuous stirring at 100 °C under N_2 until the solution became light yellow. The TG capped CdSe quantum dots were obtained at this stage. The particles were extracted by precipitation in isopropanol. The solution was stirred for one hour and the precipitate was filtered then dried in a desiccator under vacuum. Fig. 1 summarizes the mechanism of formation of TG-capped CdSe QDs.

2.2. Instrumentation

X-ray diffraction (XRD) powder spectra were taken by XPERT PRO MPD Panalytical X-ray generator using the Kα radiation of Cu at a wavelength of 1.542 Å whose integration time was monitored to improve the signal-to-noise ratio. The diffraction angle 2θ was scanned in the range 20 – 70° with a speed of 0.02 °/s. To detect the presence of TG on the surface of QDs Fourier-transform infrared (FTIR) spectra were measured using a Perkin Elmer FTIR spectrophotometer in the range 600 – 4000 cm^{-1}. For FTIR analysis, powder samples of QDs were mixed with anhydrous potassium bromide (KBr) pelletized.

For performing transmission electron microscopy (TEM) and energy dispersive X-ray (EDX) we have employed a JEOL 2010 FEG apparatus. Point EDX measurement was performed in scanning TEM mode.

2.3. Optical measurements

The UV-visible absorption spectra were collected either on a DR 5000 Hach Lange UV-vis spectrophotometer or a Shimadzu UV-1700. Fluorescence experiments were carried

out on a Cary Eclipse spectrometer and spectra were collected in the range 400 − 800 nm with an excitation at λ_{ex} = 360 nm. Absorption and emission spectra were measured at room temperature (20°C) by preparing a colloide solution of TG-CdSe quantum dots at 1.5 mg·L^{-1} in pH 8.6 buffer solution. To increase step-wise the concentration of cadmium or other transition metal ions from 1 to 24 μM, aliquots (2 – 4 μL) of a stock solution (10^{-3} M) were added into a volume of 2 mL of CdSe QDs solution and mixed thoroughly. The final dilution factor (1.024) was negligible. The temperature-dependent measurements (Supplementary Material) were carried out with a home-designed 1-mm cell holder connected to a circulating bath. The optical path-length of the quartz cuvette was 1 cm for fluorescence and 1 mm for absorption measurements. The pH measurements were carried out with a Model Hanna 8519N pH-meter and a combined glass electrode.

3. Results and discussion

3.1. Characterization of TG-capped CdSe QDs by X-ray and electronic microscopy

The XRD spectrum of TG-CdSe QDs (Fig. 2A) shows several diffraction peaks which appeared at 2θ = 25.20°, 41.90°, 49.70°, 67.96° and 77.09° corresponding to the diffraction planes (111), (220), (311), (331) and (422) respectively, according to the standard JCPDS data (card 19–0191) of bulk cubic CdSe. The peak broadening in the XRD pattern is due to a smaller size nanoparticles population. The average diameter D of the CdSe nanoparticle can be estimated from the full width at half maximum (FWHM) of the (111) diffraction peak by means of Debye-Scherrer's [26] formula:

$$D = 0.9\lambda / \beta\cos\theta \qquad (1)$$

where λ is the wavelength of the incident X-rays, β is the FWHM of the (111) peak in radians and θ is the Bragg diffraction angle. The average crystal size of the CdSe QDs thus estimated is 2.5 nm ± 0.02 nm.

An EDX analysis allowed to ascertain the composition of functionalized CdSe QDs whose spectrum (Fig. 2B) shows strong atomic peaks which originate from Cd and Se of QDs and peaks from thioglycerol ligand (S, C and O); nickel from the grid is also detected. The integration of Cd and Se signals indicates an average atomic percentage ratio Cd/Se = 32.2/23.2 = 1.39, showing that the synthesized QDs are enriched in cadmium.

Transmission electron microscopy (TEM) was employed to verify the morphology of the TG-CdSe QDs and to obtain a direct measurement of their size. The image (Fig. 3A) reveals a cluster of nanoparticles which are almost spherical and whose size population has a very small dispersion. The average diameter of nanoparticles was directly measured on high resolution TEM images (Fig. 3B) with the JEOL software and have a value of ~2.5 nm, remarkably close to the diameter calculated from the edge absorption spectrum and X-ray diffraction, which yielded 2.8 nm and 2.5 nm, respectively.

3.1. Characterization of TG-capped CdSe QDs by FT-IR and UV-visible spectroscopies

The bonding between the stabilizer thioglycerol molecules and CdSe QDs was confirmed by FT-IR measurement in the range 600 – 4000 cm^{-1} (Fig. 4). The assignments of vibrational modes are given in Table 1. This spectrum is similar to that of thioglycerol except for the absence of the S-H vibration band which appears usually at 2557 cm^{-1}, indicating that thiolate functions are connected to the Cd^{2+} sites of the CdSe nanocrystals surface [27], as observed for core-shell CdSe/CdS QDs [28], implying that thiol-assisted capping of CdSe

quantum dots has occurred. We can thus infer the presence of the organic layer coating on CdSe on the basis of the FTIR spectrum.

The UV-vis absorption spectrum is similar to that obtained for a film of TG-CdSe QDs synthesized via an organic route [29]. Both the absorption profile and first peak position (400 nm; 3.01 eV) depend upon the particle size [30] and readily indicate the small size of these CdSe nanocrystals. The absorption spectra and fluorescence spectra (Fig. 5) of TG-CdSe QDs differ from that of bulk CdSe, with an absorption edge around 400 nm clearly blue shifted as compared to CdSe (1.74 eV, 700 nm). These values indicate an increase in the band gap of the QDs after TG treatment and witness about the quantum confinement effect which becomes more pronounced when the particle size becomes less or equal to the Bohr radius of the exciton in the corresponding bulk material [31].

The absorption edge threshold (λ_{thres}) of the UV–vis absorption spectrum has been correlated with the particle diameter (D) by Henglein's [32] whose experimental curve was described by an empirical relation [33]:

$$D_{CdSe} = [1.338 - 0.002345\ \lambda_{thres}]^{-1} \text{ in nm} \quad (2)$$

One must note that this relation, which is a fit of experimental data [33], is valide only in the range ~1.5 – 6.5 nm. The absorption edge threshold (λ_{thres}) is defined as the wavelength at the inflection point of the sharply decreasing side absorption (crossing of the spectrum and its tangent), as described in Fig. 5B. This yielded the value λ_{thres} = 420 ± 1 nm, allowing to estimate the particles average diameter to be 2.83 ± 0.02 nm, very close to that calculated from the X-ray diffraction measurement (2.5 nm).

To estimate the band gap energy, the effective mass model can be used since the radius of the nanoparticles is lower than the Bohr radius of bulk exciton [34] (5.6 nm). If one neglects the energy of coulombic interaction between electron and hole which varies as $1/R$, the band gap energy of QDs can be deduced from the following equation:

$$E_g^{eff} = E_g + (h^2/8\mu R^2) \quad (3)$$

where R is the particle radius, μ the effective reduced mass, E_g the bulk band gap energy (1.74 eV), E_g^{eff} the effective band gap energy and h is the Plank's constant. Since the effective mass of electron is much smaller than that of the holes ($m_e^{eff} = 0.13\ m_0$, $m_h^{eff} = 0.45\ m_0$), the charge carrier confinement mainly affects the energetic level of the electrons. By using the estimated particle size from absorption edge threshold (2.83 nm), the calculated effective band gap of CdSe QDs is 2.21 eV.

3.2. Detection of cadmium ion and response of TG-capped CdSe nanoparticles

The optical response of TG-CdSe QDs in buffer solution (pH 8.6) has been evaluated as a function of cadmium concentration (Fig. 6A). The absorbance of the first band, initially located at 400 nm, increases with the addition of Cd^{2+} ions together with a shift of its position to 409 nm. We also observed that the band located at 365 nm in the absence of Cd^{2+} disappears as the concentration increases, while the long-tailed absorption (> 450 nm) increases. This latter change is not due to scattering from particles since the absorption increase at 450 nm is larger than at 300 nm and does not follow the proportionality with $1/\lambda^4$. This long-tailed absorption increase was also observed in the case of functionalized CdS QDs interacting with Co^{2+} ions [35]. These spectral changes are a direct consequence of the metal ions interaction with TG-CdSe QDs. To visualize the real spectral evolution, we plotted the difference spectra at a given Cd^{2+} concentration *minus* the spectrum in the absence of Cd^{2+} (Fig. 6B) which reveals the appearance of an absorption band centered at 427 nm and the shift of the small band at 373 nm to 385 nm.

The enhancement of absorbance of TG-CdSe QDs varies linearly at 427 nm with the Cd^{2+} ion concentration within the range 5.0 − 22 μM with a slope of K = 0.0278 μM^{-1} (Fig. 7)

yielding a limit of detection LOD = 0.32 µM (37 µg·L^{-1} of Cd^{2+}) defined as LOD = 3σ/K [36] where σ is the standard deviation. This value is very similar to that measured for the detection of Hg^{2+} and I^- by fluorescence quenching of triethanolamine-capped CdSe QDs [19] which, however, did not detect Cd^{2+}, whereas the present TG-CdSe QDs do not interact with Hg^{2+}, remarkably emphasizing the dependence of metal binding upon the nature of the capping chain.

The pH may affect the optical properties of functionalized QDs [37]. We indeed observed the pH-dependence of the UV-vis absorption spectra of TG-CdSe QDs in the presence of 15 µM Cd^{2+} ions over the pH range 2.0 – 12 (Fig. 7A). These measurements were expressed as the difference in absorbance of the TG-CdSe QDs in the presence and absence of Cd^{2+} at 400 nm. The maximum response $A - A_0$ at 400 nm was obtained at pH = 8.6 (Fig. 7A) whereas for pH < 6 the absorbance was too weak and vanished at pH = 2. This may be attributed to the dissociation of the TG modified CdSe nanoparticles by protonation of the surface-binding thiolates [38]. On the other hand, for pH larger than 8.6, the absorbance decreases with a simultaneous precipitation of $Cd(OH)_2$. Consequently, a standard pH of 8.6 was chosen for performing all experiments.

The response time of Cd^{2+} binding to TG-CdSe should depend on the concentration since the process can be described as a diffusion dependent receptor-ligand interaction. The kinetics of the absorbance change at 400 nm (Fig. 7B) after the addition of 15 µM Cd^{2+} to the TG-CdSe QDs solution shows that the induced change ($A-A_0$) has reached 75% of its maximum after 90 s. In order to standardize the measurements, we have chosen a 90-s response time after the addition of any metal cations at varying concentration to further characterize the TG-CdSe cation interaction.

The fluorescence intensity decreased when increasing the concentration of Cd^{2+} (Fig. 8) but without noticeable changes in the position of maximum and shape of the fluorescence

spectrum. Consequently, the presence of Cd^{2+} gave rise to a quenching of the emission of QDs, which should be more pronounced than apparently observed if we consider the increase of the absorption coefficient at 360 nm, the excitation wavelength. This apparent quenching could be partly linked to reabsorption of emission due to the increase of absorption at 570 nm and suggests a strong interaction between Cd^{2+} and TG-CdSe QDs [39]. The decrease of fluorescence observed here is at variance with the increase induced by Cd^{2+} (5 – 50 µM range) binding to CdSe/ZnS core/shell QDS caped with carnitine [40], suggesting different mechanisms for the two kinds of QDs.

As the thiol groups of TG are covalently bound to the QDs core, leaving the hydroxyl groups free, they can provide selective coordination sites for Cd^{2+} ions. On this basis, we propose in Fig. 9 a model for a working hypothesis where the cadmium cations interact with the hydroxyl groups of TG and forms cadmium oxide on the surface of CdSe QDs. We have retained the hypothesis of Cd^{2+} interacting with the non-ionized OH groups of TG rather than with their ionized form, because their pKa = 9.43 [41] and we have observed the maximal response for pH = 8.6.

We have also investigated the influence of the buffer composition, QDs concentration and temperature on the spectral properties and binding of Cd^{2+} to TG-CdSe QDs. The corresponding data are given in Supplementary Material. The various buffers used had no influence on the spectra whereas variations of the QDs concentration do not change the spectral shape and do not shift the bands. At large QDs concentration, a limited aggregation leads to an absorbance increase which is not proportional to the concentration. The absorbance edge of TG-CdSe QDs in the absence of Cd^{2+} has very slightly shifted as the temperature increased from 20 °C to 50 °C (Fig. S3). In the presence of 15 µM Cd^{2+}, there is a decrease of the absorbance from 10 to 50 °C (Fig. S3B), while disclosing the same shift of the first band maximum position to 409 nm due to Cd^{2+} binding. This dependence is less

pronounced between 10 and 20 °C and has a larger slope at 50 °C. We readily assigned this decrease to the displacement of the equilibrium of Cd^{2+} interacting with the OH groups of TG, as it must be observed for any ligand-receptor system (Fig. S3C and D). This does not affect the capability of detecting Cd^{2+}, but agrees with the origin of the absorption spectral changes assigned to Cd^{2+} binding.

3.3. Influence of foreign metal Ions nature and specificity for Cd^{2+}

The presence of interfering ions may affect the optical response due to the Cd^{2+}-TG-CdSe interaction and we have therefore examined the selectivity of this binding. Fig. 10 shows the effect of particular metal cations at fixed concentration (20 μM) on the absorption of QDs at 400 nm. Saliently, only the addition of Cd^{2+} ions led to a drastic change of the absorbance whereas no spectral change was observed after the addition of the following metal cations alone: K^{+}, Na^{+}, Li^{+}, Pb^{2+}, Ni^{2+}, Mn^{2+}, Mo^{2+}, Hg^{2+}, Zn^{2+}, Ca^{2+}, Mg^{2+}, Fe^{2+}, Cu^{2+}, Co^{2+}, Ba^{2+}, Al^{3+} and Fe^{3+}. Moreover, the simultaneous presence of these cations with Cd^{2+} in solution of TG-CdSe QDs induced a similar increase of absorption as observed for Cd^{2+} alone (Fig. 10). Therefore, there is no competition between these common ions and Cd^{2+} for the binding to TG-CdSe QDs which can thus be used as a selective probe for the Cd^{2+} ions in aqueous solution at room temperature, whatever the absence or presence of other cations.

The binding properties of TG-CdSe QDs must be compared to those of other systems. Indeed, QDs made with different materials and capped with various ligands were shown to interact with various metal cations such as Hg^{2+} [19,42] ,Cu^{2+} [43], Ba^{2+} [44], and Pb^{2+} [45]. When functionalized with 2-mercaptoethanol, CdSe QDs have been shown [44] to bind Ba^{2+} but not Cd^{2+} (no result was reported for Fe^{2+} and Cu^{2+}, which are common interfering cations). Such a difference is remarkable and may provide a future direction to investigate the

mechanism of selectivity in these systems. Not only the functionalization, but also the nature of QD itself determines the selectivity. For example, CdS QDs functionalized with carboxyl [35] is selective for Co^{2+}, whereas CdTe QDs coupled with phenol-formaldehyde resin nanoparticles detected the binding of Cu^{2+} by means of fluorescence energy transfer.

We must note that neither CdSe QDs synthesized via the organic route at high T and functionalized with bovine serum albumin [46], nor CdS QDs functionalized with carboxyl [34], nor CdTe QDs capped with phenol-formaldehyde [43] can bind Cd^{2+} ions. The large number of cations that we tested here emphasizes the selectivity of the TG-CdSe sustem as a potential optical sensor for Cd^{2+} ions, whose molecular properties and mechanism at the origin of this selectivity remain to be investigated.

4. Conclusion

In the present work, TG-capped CdSe QDs were successfully synthesized in aqueous medium, in an easy and highly reproducible way, by using safe and low cost materials. These functionalized QDs selectively detect Cd^{2+} ions even in the presence of other cations which are physiologically relevant or can be present in water as pollutants. Under defined conditions (pH = 7 – 9), this system shows sensitivity for Cd^{2+} ions in the concentration range 1.0 – 22 μM with a detection limit of 0.32 μM (37 $\mu g \cdot L^{-1}$). Together with a facile and low cost synthesis, its sensitivity and remarkable selectivity make the thioglycerol-capped CdSe a promising candidate for designing an optical tool to probe Cd^{2+} ions in solution, possibly to investigate its interaction with cultured cells.

Acknowledgements

N.B.B. acknowledges a travel research fellowship "Bourse d'Alternance" from the Tunisian Government. We thank Mélanie Poggi (Laboratoire de Physique de la Matière Condensée, Ecole Polytechnique) for her expert assistance in recording TEM images.

Appendix A. Supplementary data

Supplementary data associated with this article can be found, in the online version, at http://dx.doi.org/10.1016/j.snb.2015.07.049

Abbrevations

TG-CdSe QDs: Cadmium-Selenium Quantum Dots functionalized with Thio-Glycerol capping. TEM: Transmission Electronic Microscopy. EDX: Energy Dispersive X-ray.

References

[1] Zheng Y., Gao S., Ying J. Y. Synthesis and cell-imaging applications of glutathione-capped CdTe quantum dots. Adv. Mater. 19 (2007) 376–380.

[2] Moussodia R. O., Balan L., Merlin C., Mustin C., Schneider R. Biocompatible and stable ZnO quantum dots generated by functionalization with siloxane-core PAMAM dendrons. J. Mater. Chem. 20 (2010) 1147–1155.

[3] Costa-Fernandez J. M., Pereiro R., Sanz-Medel A. The use of luminescent quantum dots for optical sensing. TrAC–Trends Anal. Chem. 25 (2006) 207–218.

[4] Lim J., Jun S., Jang E., Baik H., Kim H., Cho J. Preparation of highly luminescent nanocrystals and their application to light-emitting diodes. Adv. Mater. 19 (2007) 1927–1932.

[5] Robel I., Subtamanian V., Kuno M., Kamat P. V. Quantum dot solar cells. Harvesting light energy with CdSe nanocrystals molecularly linked to mesoscopic TiO_2 films. J. Am. Chem. Soc. 128 (2006) 2385–2393.

[6] Jamieson T., Bakhshi R., Petrova D., Pocock R., Imani M. Biological applications of quantum dots. Biomaterials 28 (2007) 4717–4732.

[7] Aldeek F., Balan L., Medjahdi G., Roques-Carmes T., Malval J.P., Mustin C., Ghanbaja J., Schneider R. Enhanced optical properties of core/shell/shell CdTe/CdS/ZnO quantum dots prepared in aqueous solution. J. Phys. Chem. C 113 (2009) 19458–19467.

[8] Murray C. B., Norris D. J., Bawendi M. G. Synthesis and characterization of nearly monodisperse CdE (E = S Se Te) semiconductor nanocrytallites. J. Am. Chem. Soc. 115 (1993) 8706–8715.

[9] Peng X. G. Green chemical approaches toward high-quality semiconductor nanocrystals. Chem. Eur. J. 8 (2002) 335–339.

[10] Qu L., Peng Z. A., Peng X. Alternative routes toward high quality CdSe nanocrystals. Nano Letters 1 (2001) 333–337.

[11] Khanna P. K., Singh N., Charan S., Lonkar S. P., Reddy A. S., Patil Y., Viswanath A. K. The processing of CdSe/polymer nanocomposites via solution organometallic chemistry. Mater. Chem. Phys. 97 (2006) 288–294.

[12] Yu W. W., Chang E., Drezek R., Colvin V. L. Water-soluble quantum dots for biomedical applications. Biochem. Biophys. Res. Commun. 348 (2006) 781–786.

[13] Spanhel L., Haase M., Weller H., Henglein A. Photochemistry of colloidal semiconductors .20. Surface modification and stability of strong luminescing CdS particles. J. Am. Chem. Soc. 109 (1987) 5649–4655.

[14] Gaponik N., Talapin D. V., Rogach A. L., Hoppe K., Shevchenko E. V., Kornowski A., Eychmuller A., Weller H. Thiol-capping of CdTe nanocrystals: An aLernative to organometallic synthetic routes. J. Phys. Chem. B 106 (2002) 7177–7185.

[15] Rogach A. L., Kornowski A., Gao M. Y., Eychmuller A., Weller H. Synthesis and characterization of a size series of extremely small thiol-stabilized CdSe nanocrystals. J. Phys. Chem. B 103 (1999) 3065–3069.

[16] Xue X. H., Pan J., Xie H. M., Wang J. H., Zhang S. Fluorescence detection of total count of Escherichia coli and Staphylococcus aureus on water-soluble CdSe quantum dots coupled with bacteria. Talanta 77 (2009) 1808–1813.

[17] Su B., Fermin D. J., Abid J. P., Eugster N., Girault H. H. Adsorption and photoreactivity of CdSe nanoparticles at liquid/liquid interfaces. J. Electroanal. Chem. 583 (2005) 241–247.

[18] Bin Shang Z., Wang Y., Jin W. J. Triethanolamine-capped CdSe quantum dots as fluorescent sensors for reciprocal recognition of mercury [II] and iodide in aqueous solution. Talanta 78 (2009) 364–369.

[19] Nazzal A. Y., Qu L., Peng X., Xiao M. Photoactivated CdSe nanocrystals as nanosensors for gases. Nano Letters 3 (2003) 819-822.

[20] Chaney R. L., Ryan J. A., Li Y. M., Brown S. L., McLaughlin M. J., Singh B. R. Eds. In Cadmium in soils and plants. Kluwer: Boston 1999, 219−246.

[21] Nordberg G. F., Herber R. F. M., Alessio L. Cadmium in the human environment, Oxford University Press: Oxford UK 1992.

[22] Friberg L., Elinger C. G., Kjellstrom T. Cadmium. World Health Organization Report: Geneva 1992.

[23] Goyer R. A., Liu J., Waalkes M. P. Cadmium and cancer of prostate and testis. BioMetals 17 (2004) 555−558.

[24] Satarug S., Baker J. R Urbenjapol S., Haswell-Elkins M., Reilly P. E., Williams D. J., Moore M. R. A global perspective on cadmium pollution and toxicity in non-occupationally exposed population. Toxicol. Lett. 137 (2003) 65−68.

[25] Bel Haj Mohamed N., Haouari M., Zaaboub Z., Nafoutti M., Hassen F., Maaref H., Ben Ouada H. Time resolved and temperature dependence of the radiative properties of thiol-capped CdS nanoparticles films. J. Nanopart. Res. 16 (2014) 2242. DOI 10.1007/s11051-013-2242-9

[26] Deng Z., Cao L., Tang F., Zou B. A new route to zinc-blende CdSe nanocrystals: mechanism and synthesis. J. Phys. Chem. B 109 (2005) 16671–16675.

[27] Tang H., Yan M., Zhang H., Xia M., Yang D. Preparation and characterization of water-soluble US nanocrystals by surface modification of ethylene diamine. Mater. Lett. 59 (2005) 1024–1027.

[28] Silva A. C. A., Da Silva S. W., Morais P. C., Dantas N. O. Shell thickness modulation in ultrasmall CdSe/CdS_xSe_{1-x}/CdS core/shell quantum dots via 1-thioglycerol. ACS Nano 8 (2014) 1913−1922.

[29] Artemyev M. V., Woggon U., Jaschinski H., Gurinovich L. I., Gaponenko S. V. Spectroscopic study of electronic states in an ensemble of close-packed CdSe nanocrystals. J. Phys. Chem. B 104 (2000) 11617-11621.

[30] Jasieniak J., Smith L., van Embden J., Mulvaney P., Califano M. Re-examination of the Ssize-dependent absorption properties of CdSe quantum dots. J. Phys. Chem. C 113 (2009) 19468–19474.

[31] Cao Y. C., Wang J. H. One-Pot Synthesis of high-quality zinc-blende CdS nanocrystals. J. Am. Chem. Soc. 126 (2004) 14336–14337.

[32] Spanhel L., Haase M., Weller H., Henglein A. Photochemistry of colloidal semiconductors. 20. surface modification and stability of strong luminescing CdS particles. J. Am. Chem. Soc. 109 (1987) 5649−5655.

[33] Moffitt M., Eisenberg A. Size control of nanoparticles in semiconductor-polymer composites. 1. control via multiplet aggregation numbers in styrene-based random ionomers. Chem. Mater. 7 (1995) 1178−1184.

[34] Brus L. E. Electron-electron and electron-hole interactions in small semiconductor crytallites: the size dependence of the lowest excited electronic state. J. Chem. Phys. 80 (1984) 4403–4409.

[35] Gore A. H., Gunjal D. B., Kokate M. R., Sudarsan V. P., Anbhule V., Patil S. R., Kolekar G. B. Highly Selective and sensitive recognition of cobalt[II] ions directly in aqueous solution using carboxyl-functionalized CdS quantum dots as a naked eye colorimetric probe: applications to environmental analysis. ACS Appl. Mater. Interfaces 4 (2012) 5217–5226.

[36] Chen J., Zheng A., Gao Y., He C., Wu G., Chen Y., Kai X., Zhu C. Functionalized US quantum dots-based luminescence probe for detection of heavy and transition metal ions in aqueous solution. Spectrochimica Acta A 69 (2008) 1044–1052.

[37] Skoog D. A., Holler F. J., Nieman T. A. Principles of instrumental analysis 7th ed. Saunders College Philadelphia 1998 601–608.

[38] Biju V., Makita Y., Sonoda A., Yokoyama H., Baba Y., Ishikawa M. Temperature-sensitive photoluminescence of CdSe quantum dot clusters. J. Phys. Chem. B 109 (2005) 13899–13905.

[39] Lakowicz J. R., Gryczynski I., Gryczynski Z., Murphy C. J. Luminescence spectral properties of CdS nanoparticles. J. Phys. Chem. B 103 (1999) 7613–7620.

[40] Li H., Zhang Y., Wang X. L-Carnitine capped quantum dots as luminescent probes for cadmium ions. Sens. Actuators B 127 (2007) 593–597.

[41] Xu S., Wang C., Zhang H., Wang Z., Yang B., Cui Y. pH-sensitive photoluminescence for aqueous thiol-capped CdTe nanocrystals. Nanotechnology 22 (2011) 315703.

[42] Chen B., Ying Y., Zhou Z. T., Zhong P. Synthesis of novel nanocrystals as fluorescent sensors for Hg^{2+} ions. Chem. Letters 33 (2004) 1608−1609.

[43] Yang P., Zhao Y., Lu Y., Xu Q. Z., Xu X. W., Dong L., Yu S. H. Phenol formaldehyde resin nanoparticles loaded with CdTe quantum dots: a fluorescence resonance energy transfer probe for optical visual detection of copper(II) ions. ACS Nano 5 (2011) 2147−2154.

[44] Mahmoud W. E. Functionalized ME-capped CdSe quantum dots based luminescence probe for detection of Ba^{2+} ions. Sens. Actuators B 164 (2012) 76–81.

[45] Wu H., Liang J., Han H. A novel method for the determination of Pb^{2+} based on the quenching of the fluorescence of CdTe quantum dots. Microchim. Acta 161 (2008) 81−86.

[46] Liang J.-G., Ai X.-P., He Z.-K., Pang D.W. Functionalized CdSe quantum dots as selective silver ion chemodosimeter. Analyst 129 (2004) 619–622.

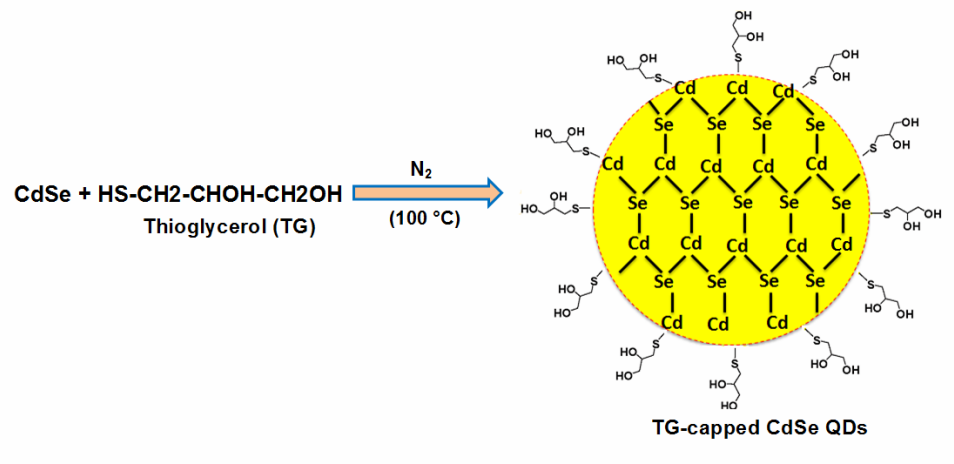

Fig. 1. Summary of TG-capped CdSe QDs synthesis via the aqueous route.

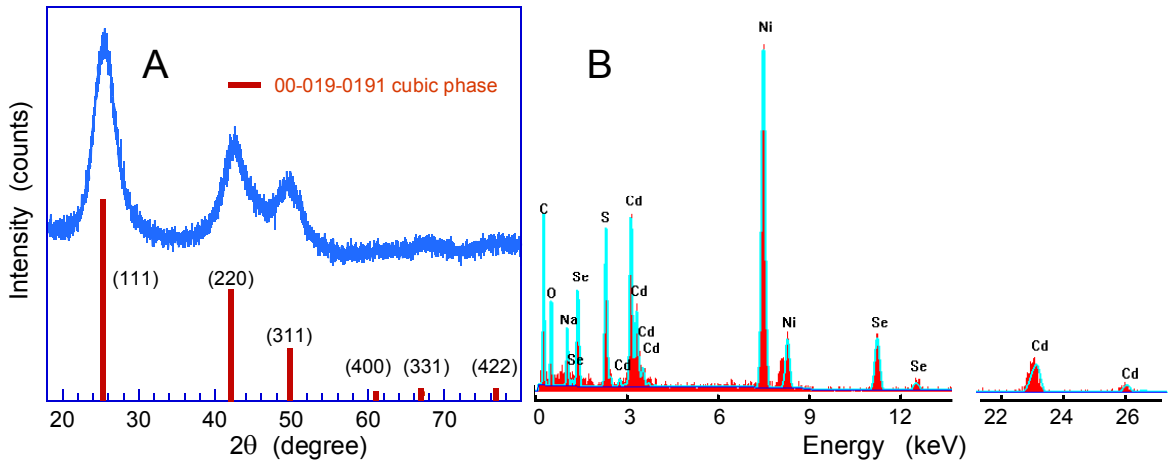

Fig. 2. (A) X-ray diffraction pattern for the TG-CdSe QDs. The positions of the corresponding cubic phases are indicated. (B) The EDX spectrum of TG-CdSe QDs and the reference atomic pattern are displayed in red and blue, respectively.

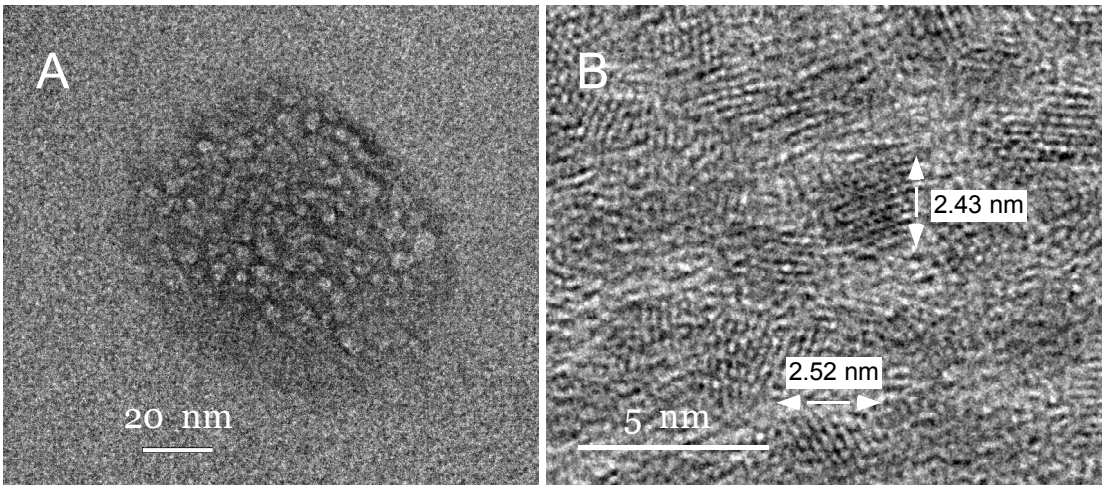

Fig. 3. (A) TEM image of a cluster of TG-CdSe QDs. (B) High resolution and large magnification (× 600 000) image of individual TG-CdSe nanoparticles whose size was estimated by using the software DigitalMicrograph (Jeol).

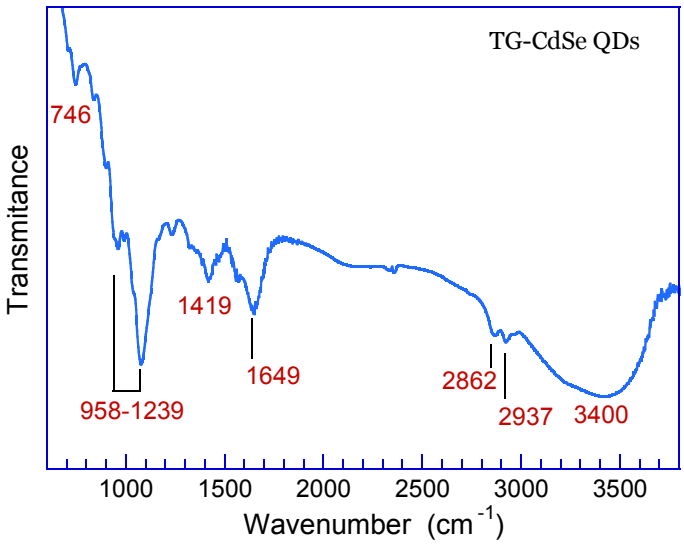

Fig. 4. Fourier transform infrared spectrum of TG-CdSe QDs mixed with anhydrous KBr. The band assignments are indicated in Table 1.

Table 1. Assignment of the bands in the FT-IR spectrum of TG-CdSe QDs.

Wavenumber (cm^{-1})	**Assignment**
746	Cd-Se bond stretching
958, 1083 and 1239	C-C stretching modes
1419	C-H stretching mode
1649	O-H bending mode of water
2862	C-H stretching mode
2937	CH_2 symmetric stretching
3400	O-H stretching mode

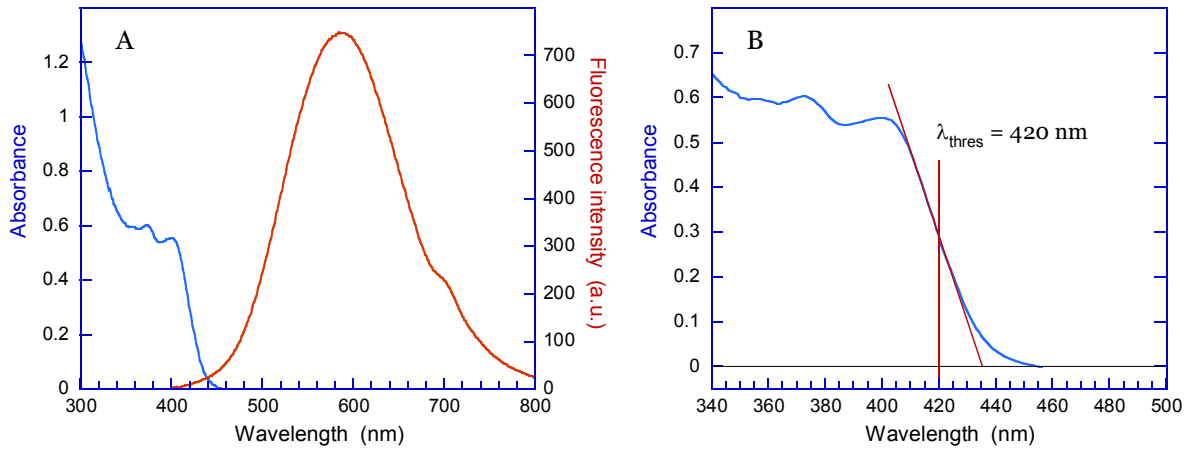

Fig. 5. (A) UV-visible absorption and fluorescence spectra of functionalized TG-CdSe QDs in aqueous solution. (B) Absorption edge threshold used for estimating the diameter of TG-CdSe QDs according to Henglein's empririal relation.

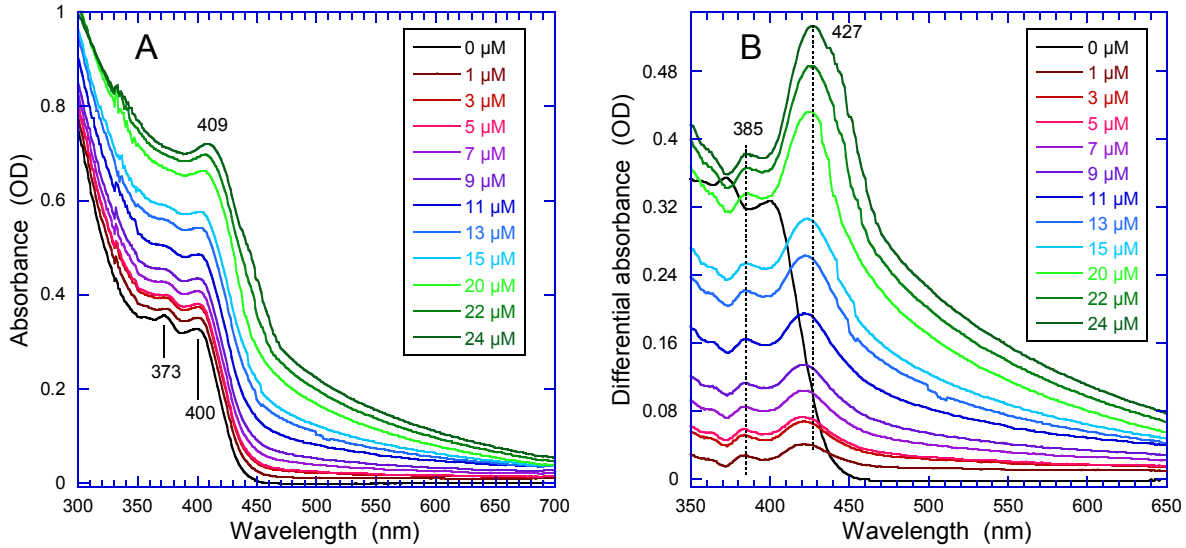

Fig. 6. (A) UV-vis absorption spectra of the TG-CdSe QDs (5×10^{-4} M) solution with various concentrations of Cd^{2+} ions at equilibrium. (B) Difference absorption spectra at increasing Cd^{2+} concentration *minus* the spectrum of TG-CdSe QDs in absence of Cd^{2+}. pH = 8.6.

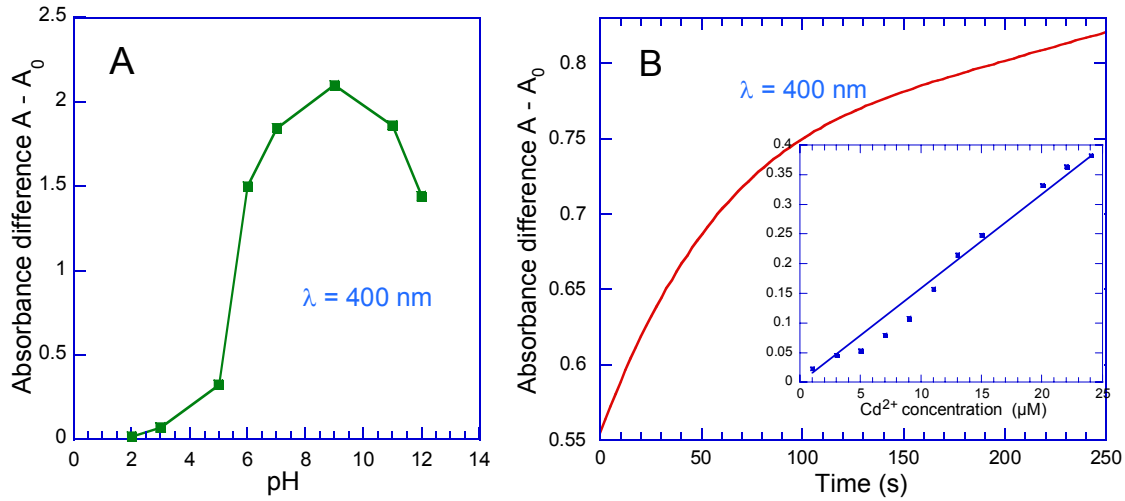

Fig. 7. (A) pH-dependent changes of the absorbance difference at 400 nm of the TG-CdSe QDs (5×10^{-4} M) solution in the presence Cd^{2+} ions (15 μM). (B) Kinetics of the absorption response at 400 nm of the TG-CdSe QDs (5×10^{-4} M) solution at pH = 8.6 mixed with Cd^{2+} ions (15 μM). Inset: dependence of $(A - A_0)$ at 400 nm on the Cd^{2+} ions concentration, with a linear fit (correlation coefficient = 0.9923). A and A_0 are the absorbance of TG-CdSe QDs in presence and in absence of Cd^{2+} ions respectively.

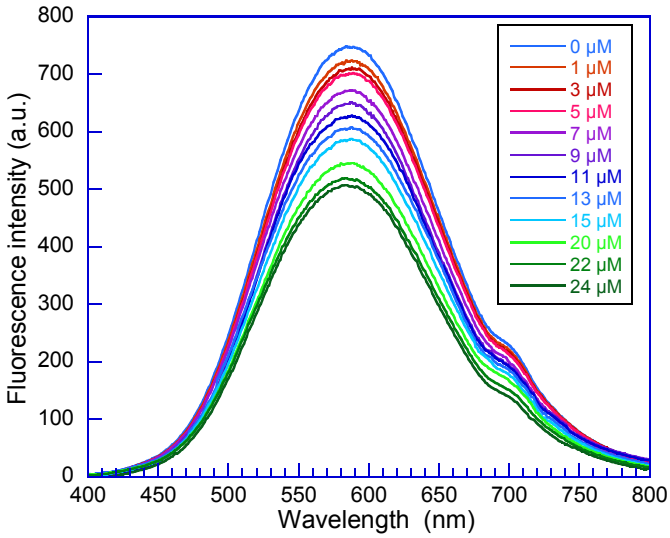

Fig. 8. Evolution of the fluorescence spectrum of TG-CdSe QDs (5×10^{-4} M) after the addition of increasing concentration of Cd^{2+}. Excitation wavelength is 360 nm.

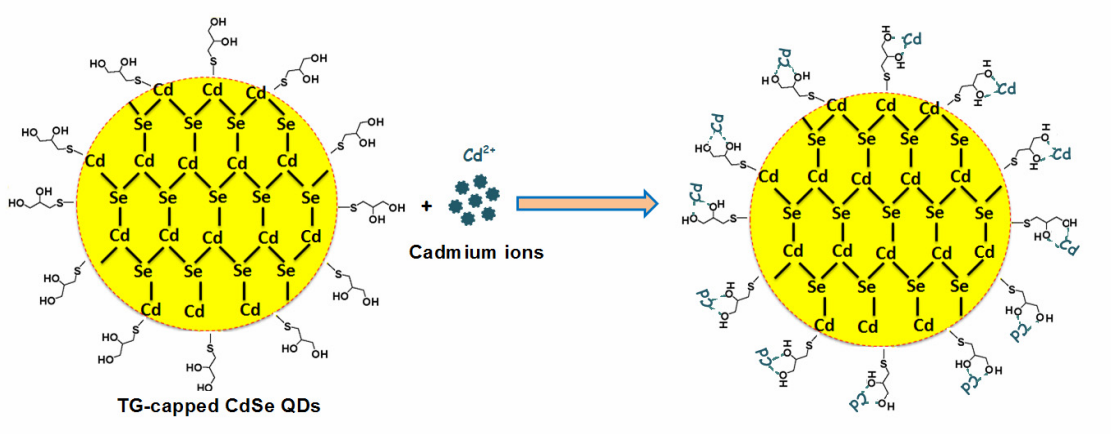

Fig. 9. Proposed mechanism of interaction between TG-capped CdSe QD and Cd^{2+} ions.

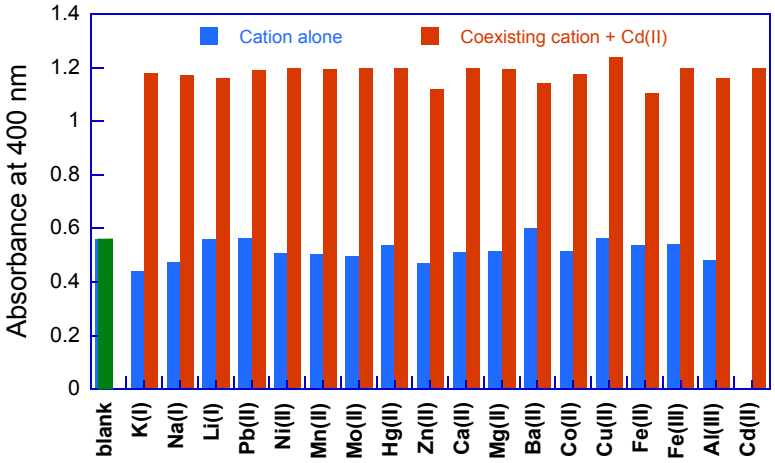

Fig. 10. Absorption intensity of the TG-CdSe QDs (5×10^{-4} M) solution at 400 nm shows specificity for Cd^{2+} ion. Blue bars denote the response of QDs to various individual metal cations (20 μM) and orange bars show the response in the simultaneous presence of Cd^{2+} (15 μM) and various coexisting ions.

Grapical Abstract: